# Radio frequency generation of an electron plasma in the Malmberg-Penning trap ELTRAP

M. Romé[1], F. De Luca[1], G. Maero[1], B. Paroli[1,2], R. Pozzoli[1]

[1] *I.N.F.N. Sezione di Milano and Dipartimento di Fisica, Università degli Studi di Milano, Italy*

[2] *Dipartimento di Energia, Politecnico di Milano, Italy*

High powers are generally used in plasma sources to induce a discharge in relatively high-pressure neutral gases ($10^{-3}$ – 10 mbar) [1]. A different generation mechanism is presented here, where an electron plasma is formed within a Malmberg-Penning trap [2] under ultra-high vacuum (UHV) conditions (few $10^{-9}$ mbar base pressure) by means of the application of a low-power radio frequency (RF) drive on one of the trap electrodes.

The study has been conducted in the ELTRAP device [3] (see Fig. 1). The application of potentials up to -100 V on two given electrodes allows axial trapping of electrons, while a surrounding solenoid creates an axial magnetic field up to 0.2 T responsible for the radial confinement. For the generation of the electron plasma sinusoidal waveforms of amplitude and frequency up to 10 V and 80 MHz, respectively, are applied on one of the electrodes [4]. After a given time the plasma is dumped on a phosphor screen kept at a high positive voltage (+15 kV) by lowering the potential on the closest trapping electrode. The intensity of the light emitted by the phosphor and detected by a CCD camera is proportional to the axially-integrated electron density. Fig. 2 shows a series of shots taken for increasing time periods of RF application. The formation of the plasma is appreciably detected after $\approx$ 300 ms. The plasma is produced mainly close to the trap wall and as time progresses fills the central region of the trap. This can be due to plasma production near the axis as well as to other mechanisms (e.g. diffusion, compression modes) whose role and interplay are presently under study.

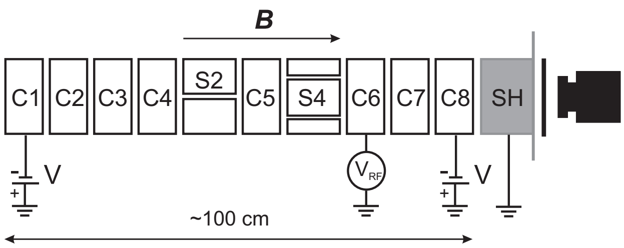


Figure 1: Scheme of the ELTRAP set-up, with a CCD camera for the optical diagnostics. The electrodes have an inner diameter of 9 cm and are 9 cm (C1 to C8) or 15 cm (S2 and S4) long. Electrodes S2 and S4 are split into two and four azimuthal sectors, respectively.

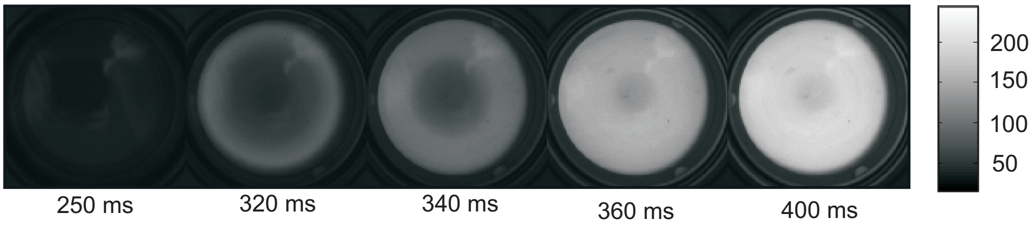


Figure 2: CCD camera shots of the axially-integrated transverse density during the early formation stage. Electrodes C1 and C8 were biased to a potential of -80 V and a RF drive of amplitude 3.8 V and frequency 8 MHz was applied to electrode C7.

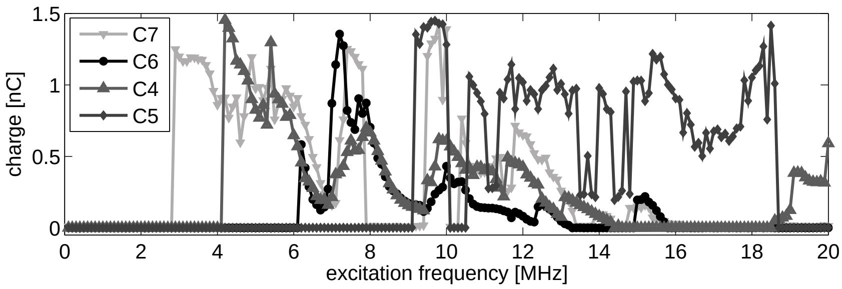


Figure 3: Total charge after 4.5 s of RF application versus the frequency of the RF drive. The plasma is formed and confined between the electrodes C1 and C8. The legend specifies the electrode used as antenna for the RF excitation.

After a few seconds of continuous RF excitation the total charge produced and confined in the trap remains constant as an effect of the dynamical equilibrium between ionization and losses. The amount of charge is influenced by the RF parameters as well as by the geometry of the trap. In the experiments the drive frequency was changed in the interval 0.1-20 MHz, different confinement lengths were used and several electrodes were chosen as excitation antennas. The results for a *long* (C1-C8) trap are summarized in Fig. 3. The plasma was generated by the continuous application of an RF drive of 3.8 V amplitude for 4.5 s and then downloaded on the phosphor screen, used as a charge collector. Total charges up to 1.5 nC were obtained, with densities of some $10^6$ cm$^{-3}$. The plasma production scheme thererefore offers an interesting alternative to the widely used thermocathode sources [2] in low-energy non-neutral plasma applications. An appreciable formation of plasma is detected beyond a certain threshold frequency which changes with the geometrical parameters, and occurs in broad frequency bands rather than resonance peaks.

The plasma build-up comes as a result of the RF heating of a seed electron population and subsequent ionization of the residual gas. Hence the kinetic energy acquired by the electrons

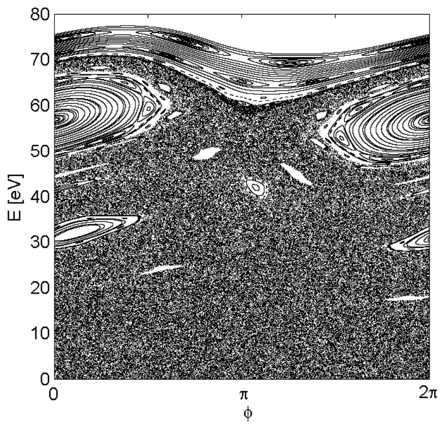


Figure 4: Plot of the energy vs the RF drive phase for $4 \cdot 10^5$ interactions of an electron with an oscillating barrier of amplitude 3.8 V and frequency 8 MHz. Several runs with different initial energies (10 meV to 75 eV) have been considered. The geometrical parameters used in the map reflect those of the experiments, with confinement between electrodes C1 and C8, and RF drive on electrode C7.

must exceed the first ionization energy for light gases, i.e. roughly 10-20 eV. This electron heating mechanism has been modeled with the use of a simple one-dimensional iterative map [4]. The particles are assumed to be trapped within a square potential well of depth $V$. The application of a RF drive to an inner electrode is modeled as a sinusoidally oscillating nested square well. An electron therefore travels at constant velocity within the three subregions defined by the ends of the trap (where the particle bounces elastically) and the extremities of the electrode on which the RF drive is applied. At the latter points, depending on the electron energy and the instantaneous value of the oscillating potential, the particle is either reflected back or moves forward with a different energy. The map shows a behavior similar to that of the Fermi acceleration model [5]. Fig. 4 plots the particle energy $E$ as a function of the phase $\phi$ of the RF drive at the inversion point on the left end of the trap. The region of the phase space is bounded by invariant spanning curves at high energy, while the low-energy region shows the presence of a "chaotic sea", and energies up to several tens of eV can be reached starting from a very low initial energy.

The electron heating process has been analyzed also by means of a two-dimensional (2D) particle-in-cell (PIC) code [6]. The code computes the dynamics of a very low density population of electrons at room temperature trapped within two cylindrical electrodes and under the effect of a sinusoidally varying potential perturbation applied on a given internal cylindrical conductor. Realistic geometrical and physical parameters can be used in the simulations. The

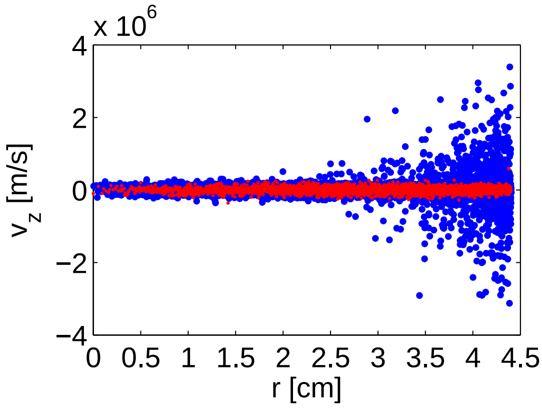


Figure 5: Radial distribution of the axial velocity of the electrons obtained from 2D PIC simulations, after 20 $\mu$s of application of a RF drive with 3.8 V amplitude and 6 MHz frequency. The magnetic field is 0.03 T. An initial spatially uniform distribution of electrons inside the trap with a density of 50 cm$^{-3}$ and a temperature $T = 0.025$ eV is considered. The blue and red dots refer to a "long" trap (-80 V on C1 and C8) with the RF applied on electrode C7, and to a "short" trap (-80 V on C1 and C5) with the RF applied on C2, respectively.

RF heating turns out to be more effective close to the conducting boundaries, as a consequence of the radial dependence of the applied electric field perturbation (see Fig. 5). In other words, electrons localized in the outer radial part of the trap are able to reach in a shorter time energies $\gtrsim$ 20 eV (allowing them to ionize the residual gas, a process not simulated here) than electrons close to the axis. These results point therefore in the same direction as the experimental findings about the plasma formation taking place initially close to the trap wall.

This work was partially supported by the Italian Ministry for University and Scientific Research "PRIN-2007" funds and by the Italian Space Agency contract I/R/98/01.

## References

[1] H. Conrads and M. Schmidt, Plasma Sources Sci. Technol. **9**, 441 (2000).

[2] J. H. Malmberg and J. S. deGrassie, Phys. Rev. Lett. **35**, 577 (1975).

[3] M. Amoretti *et al.*, Rev. Sci. Instrum. **74**, 3991 (2003).

[4] B. Paroli, F. De Luca, G. Maero, R. Pozzoli, and M. Romé, Plasma Sources Sci. Technol. **19**, 045013 (2010).

[5] A. J. Lichtenberg and M. A. Lieberman, Regular and Stochastic Motion (Springer-Verlag, New York, 1983).

[6] J. P. Verboncoeur, A. B. Langdon, and N. T. Gladd, Comp. Phys. Comm. **87**, 199 (1995).